Available online at www.sciencedirect.com
SCIENCE DIRECT®
Journal of Pharmaceutical and Biomedical Analysis
35 (2004) 1113–1125
JOURNAL OF PHARMACEUTICAL AND BIOMEDICAL ANALYSIS
www.elsevier.com/locate/jpba

Degradation of camptothecin-20(*S*)-glycinate ester prodrug under physiological conditions

Xinli Liu [a], Junhong Zhang [b], Lin Song [b], Bert C. Lynn [a,*], Thomas G. Burke [b]

[a] *Department of Chemistry, University of Kentucky, Room A053, ASTeCC Building, Lexington, KY 40506, USA*
[b] *Pharmaceutical Sciences, University of Kentucky, Lexington, KY 40506, USA*

Received 25 January 2004; received in revised form 9 April 2004; accepted 13 April 2004

Available online 10 June 2004

Abstract

We have compared the strikingly different decomposition pathways for camptothecin-20(*S*)-acetate -acetate and camptothecin-20(*S*)-glycinate in phosphate buffered saline, human plasma and blood. The aliphatic ester analog camptothecin-20(*S*)-acetate demonstrated excellent stability in the above fluids for many hours with minimal hydrolysis, while the camptothecin-20(*S*)-glycinate analog (differing solely by the presence of an amino group) underwent rapid and essentially complete decomposition. Reversed-phase high performance liquid chromatography (RP-HPLC) with electrospray ionization–mass spectral (ESI–MS) detection was then used to correlate structural information for camptothecin-20(*S*)-glycinate decomposition products. ESI–MS detection indicated the ring-opened carboxylate form of camptothecin and the ring-opened degradation product co-elute near the solvent front, while the latest eluting decomposition product was the closed-ring lactone form of camptothecin. A novel decomposition product with intermediate retention time displayed an identical mass-to-charge ratio as camptothecin-20(*S*)-glycinate ester but a strikingly different fragmentation pattern. The LC–ESI–MS evidence of a novel camptothecin prodrug degradation pathway is provided in this report.

Keywords: Topoisomerase I; Camptothecin; Prodrug; Decomposition; HPLC; Electrospray ionization–mass spectrometry

1. Introduction

The antitumor activity of the topoisomerase I inhibitor 20(*S*)-camptothecin (CPT, Fig. 1), a plant alkaloid isolated from *Camptotheca acuminata*, has been well studied for over 30 years. Historically, clinical development of camptothecin (as well as other potent but water-insoluble analogs such as 10,11-methylenedioxycamptothecin, Fig. 1) has been hampered by an industrial bias favoring analogs displaying high water solubility, suitability for intravenous administration. Two such water-soluble camptothecin analogs, topotecan and CPT-11 (Fig. 1), have gained FDA approval. Prodrug development has long been recognized as an effective approach to increasing the aqueous solubility of

Abbreviations: CPT, camptothecin; CPT-20(*S*)-glycinate, camptothecin-20(*S*)-glycinate; CPT-20(*S*)-acetate, camptothecin-20(*S*)-acetate; PBS, phosphate buffered saline; LC/ESI/MS, liquid chromatography electrospray ionization–mass spectrometry; RP-HPLC, reversed-phase high performance liquid chromatography

* Corresponding author. Tel.: +1-859-257-2300x287; fax: +1-859-257-2489.
E-mail address: bclynn2@uky.edu (B.C. Lynn).

0731-7085/$ – see front matter © 2004 Elsevier B.V. All rights reserved.
doi:10.1016/j.jpba.2004.04.006

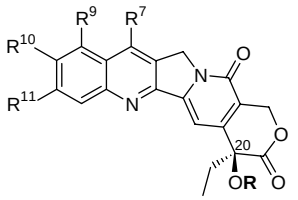

Compound	R^7	R^9	R^{10}	R^{11}	R
Camptothecin	H	H	H	H	H
Topotecan	H	$CH_2NH(CH_3)_2$	OH	H	H
CPT-11	C_2H_5	H	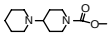	H	H
10,11-methylenedioxy-camptothecin	H	H			H
DB-67	$Si(CH_3)_2C(CH_3)_3$	H	OH	H	H
CPT-20(*S*)-acetate	H	H	H	H	$COCH_3$
CPT-20(*S*)-glycinate	H	H	H	H	$COCH_2NH_2$

Fig. 1. Chemical structures of CPT and its analogs.

agents containing a hydroxyl group, and the synthesis of more water-soluble 20-glycinate hydrochloride ester prodrugs of camptothecin and 10,11-methylenedioxycamptothecin have been described [1,2]. Since the (*S*)-α-hydroxy-δ-lactone moiety contained in these compounds is a crucial structural feature [3,4] required for biological activity, esterification creates a non-toxic prodrug. The 20(*S*)-glycinate ester prodrugs of camptothecin (CPT-20(*S*)-glycinate, Fig. 1) and 10,11-methylenedioxycamptothecin are known to chemically react in buffer and plasma to release the respective active agent, and release of active agent in vivo is also supported by the finding that the administration of the glycinate ester forms of both camptothecin and 10,11-methylenedioxycamptothecin in murine xenograft models are highly effective in treating human cancers [5].

The interest of our laboratory in the development of controlled release systems for camptothecins led us to study the details of the decomposition pathway for CPT-20(*S*)-glycinate in phosphate buffered saline (PBS), human plasma and blood [6]. Whereas the aliphatic ester analog camptothecin-20(*S*)-acetate (CPT-20(*S*)-acetate, Fig. 1) demonstrated excellent stability in the above fluids over a time course of several hours, the CPT-20(*S*)-glycinate analog (differing solely by the presence of an amino group) was found to undergo rapid and essentially complete decomposition over a similar time frame. The extent and rate of decomposition for CPT-20(*S*)-glycinate was found to be highly pH-dependent, with the prodrug exhibiting excellent stability at low pH but extensive reactivity at pH 7.4. Reversed-phase high performance liquid chromatography (RP-HPLC) with both UV and fluorescence detection demonstrated that CPT-20(*S*)-glycinate, in solution at pH 7.4, decomposes to yield new peaks attributed to decomposition products displaying different retention times relative to CPT-20(*S*)-glycinate ester prodrug. RP-HPLC with electrospray ionization-mass spectral (ESI–MS) detection was then used to correlate structural information with the new peaks caused by prodrug decomposition. Here, we report the LC–ESI–MS evidence of a novel camptothecin prodrug degradation pathway and its implications in the controlled release of active camptothecin.

2. Materials and methods

2.1. Chemicals

CPT was purchased from Sigma (St. Louis, MO). CPT-20(*S*)-glycinate ester (trifluoracetic acid salt) and CPT-20(*S*)-acetate were synthesized according to the published procedure [2]. Each agent was of high purity (>98%) as determined by TLC and HPLC

chromatographic assays using fluorescence detection. Stock solutions of the drugs were prepared in dimethylsulfoxide (DMSO) (ACS spectrophotometric grade, Aldrich, Milwaukee, WI) at a concentration of 2 mM and stored in the dark at −20 °C. All other chemicals used in the study were reagent grade and used without further purification. High-purity water provided by a milli-Q UV PLUS purification system (Bedford, MA) was utilized in all experiments. Whole human blood was obtained from a healthy male donor by drawing blood into sterile vacutainers containing either ethylenediaminetetraacetic acid (EDTA) or heparin to prevent clot formation. Human plasma was obtained from Red Cross of University of Kentucky and used without further processing. Human plasma samples for drug analysis studies were warmed to body temperature (37 °C) and constant pH (7.4 ± 0.1) was maintained by continuously aerating with "blood gas" (MEDIBLEND, Linde Medical Gases, CT, major components CO_2 and O_2).

2.2. Liquid chromatography (LC) with fluorescence and UV detection

For the analysis of CPT-20(*S*)-acetate, CPT-20(*S*)-glycinate and its degradation products , an Alliance 2690 model HPLC system equipped with a Waters 510 HPLC pump, Waters 476 fluorescence detector (excitation and emission were set at 370 and 460 nm, respectively) and Waters 486 UV–vis detector (wavelength 370 nm) was used. Chromatographic separations were carried out using a Symmetry C_{18} 5 μm particle-size reversed-phase 150 mm × 3.9 mm i.d. column at 37 °C. A binary mobile phase consisted of a mixture of acetonitrile and 2% (v/v) triethylamine acetate buffer pH 5.5 (v/v 36/65 and 26/74 for CPT-20(*S*)-acetate and CPT-20(*S*)-glycinate, respectively) and delivered at a flow rate of 1 mL/min.

2.3. Prodrug stability tests

To evaluate the conversion of prodrugs CPT-20(*S*)-acetate and CPT-20(*S*)-glycinate ester to their parent CPT compound in aqueous solution, drug stability was measured by HPLC with fluorescence detection. A 1 μM solution of each analogue was prepared by diluting a DMSO stock solution of each into PBS, pH 7.4, 37 °C. Samples were analyzed at 1, 10, 20, 30, 60, 120 and 180 min with the aid of an autosampler. The effect of pH on stability of CPT-20(*S*)-glycinate was evaluated in autosampler vials for over 3 h as described above. Drug concentrations were 1 μM, and buffer (0.1 M) pHs were 3.0 (formate), 5.0 (acetate), 6.0 (citrate) and 7.4 (phosphate) with the same ionic strength. Drug stability in biological fluids such as whole human blood and plasma was evaluated by using the well documented chilled methanol extraction and deproteinization method [7]. Solutions of drugs at concentrations of 1 μM in whole human blood and plasma (aerated with blood gas) were prepared and incubated in a 37 °C water bath. Immediately after the drug stock solution was mixed with samples and at predetermined time intervals, 100 μL aliquots each solution were taken and extracted with 400 μL chilled methanol (approximately −20 °C) with vigorous vortex mixing for 30 s. Following centrifugation at 8000 × *g* for 1 min, supernatants were directly injected HPLC using 10 μL injection volumes. Stability profile graphs were constructed by plotting the fractional percent of each species (CPT, CPT-20(*S*)-acetate and CPT-20(*S*)-glycinate) decayed over a time course. The fractional percentage of each starting material was calculated based on the ratio of the peak area of analyte at 1, 10, 20, 30, 60, 120 and 180 min versus the initial peak area. Each stability profile represents the average of at least three independent runs with the same sampling schedules. The standard deviation of each point is typically 5% or less.

2.4. LC–ESI–MS instrumentation

The LC–ESI–MS system consisted of an HP 1100 HPLC equipped with a 50 mm × 1.0 mm i.d. (3 μM) Luna C18 microbore column (Phenomex, Torrence, CA). Isocratic separations were performed at 35 μL/min using 80% acetonitrile and 20% of 10 mM ammonium formate, pH 5.5. Salts in the samples were diverted from the mass spectrometer during the first 2 min of each experiment. Electrospray mass spectra were acquired on a Finnigan LCQ Classic (San Jose, CA) quadrupole ion trap mass spectrometer in the positive ion mode. Standard electrospray conditions were used (spray voltage 4.5 kV, sheath gas flow rate 60 arbitrary units, and capillary temperature 225 °C). Full scan mass spectral range was *m/z* 100–1000. The relative collision energies for MS/MS analyses were 35%.

2.5. LC–ESI–MS sample preparation

Ten microliters of 0.4 mM CPT-20(*S*)-glycinate ester DMSO stock solution were added to 790 μL aqueous solution (pH was adjusted to 7.4 with ammonium hydroxide and formic acid) to achieve 5 μM final concentration. After hydrolyzing at room temperature for about 90 min, a 10 μL aliquot was injected. Similarly, 5 μM CPT standards (both lactone and carboxylate form of CPT) were prepared by spiking 10 μL of 0.4 mM CPT DMSO stock solution into 790 μL aqueous solutions (pH 3 and 10, respectively).

3. Results and discussion

3.1. Comparison of the stability of the CPT-20(S)-acetate and CPT-20(S)-glycinate ester

The intrinsic chemical reactivity of the lactone moiety is necessary for the biological activity of the CPT. However, it is well known that the CPT lactone moiety undergoes a spontaneous reversible hydrolysis in aqueous solutions (including blood) under neutral and alkaline pH producing a dynamic equilibrium between the closed ring of lactone (lactone form of CPT) and opened-ring carboxylic acid forms (carboxylate form of CPT). The lactone form of CPT predominates at acidic pH and carboxylate at neutral and alkaline pH. Reversible hydrolysis of the lactone ring has major implications in therapeutic efficacy because the carboxylate form of CPT is about 10-times less potent than the intact lactone. Under physiological condition the equilibrium favors the essentially less potent carboxylate form of CPT which results in a virtual loss of biological activity of CPT [8–10]. The 20-hydroxyl functional group appears to be largely responsible for the lability of the lactone ring. The formation of a hydrogen bond between the hydroxyl group and the carbonyl of the lactone facilitates hydrolytic ring opening [11]. Zhao H. et al. [12] have reported that at physiological pH 7.4, 20-*O*-acyl derivatives of CPT were substantially more stable in the lactone form than the 20-OH parent. CPT-20-*O*-ester derivatives CPT-20(*S*)-acetate and CPT-20(*S*)-glycinate were synthesized and their stabilities were evaluated in pH 7.4 PBS buffer at 37 °C in order to determine if those agents can rapidly convert to the active parent drug.

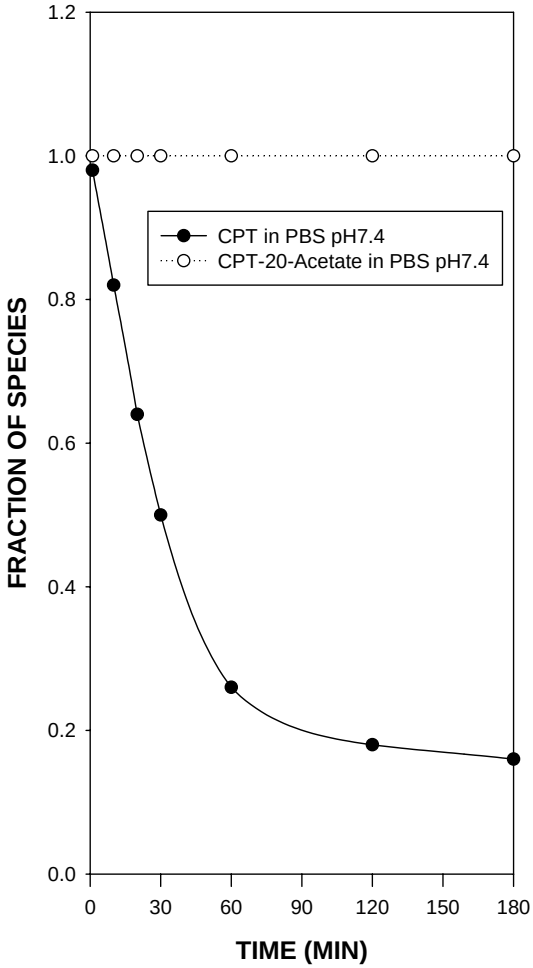

Fig. 2. Comparison of the stability of CPT and CPT-20(*S*)-acetate in PBS (pH 7.4, 37 °C).

We observed that the CPT-20(*S*)-acetate was resistant to chemical degradation in aqueous solutions at physiological pH (with negligible hydrolysis for days), and therefore, did not release parent CPT in neutral media. Fig. 2 compares the stability profile of CPT and CPT-20(*S*)-acetate in PBS, pH 7.4, 37 °C for 3 h. This result indicated that CPT-20(*S*)-acetate is resistant to chemical activation, and enzyme-mediated activation might be required to generate significant levels of active CPT in vivo.

In contrast, amine containing CPT-20(*S*)-glycinate ester is much more reactive in comparison to its corresponding aliphatic ester analogs. Dissolution of

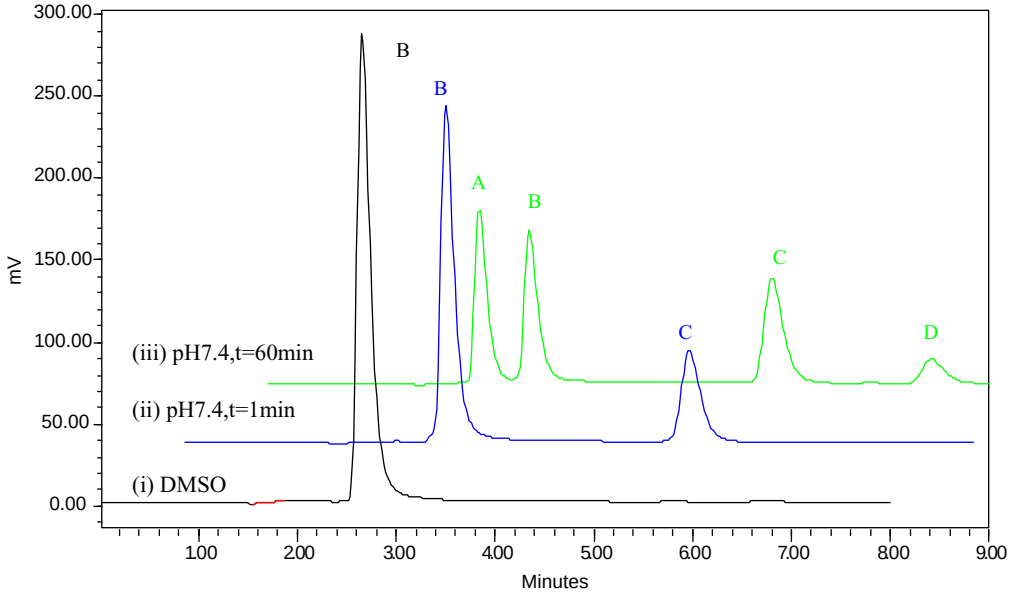

Fig. 3. Stacked plot of chromatograms of CPT-20(*S*)-glycinate hydrolysate taken in PBS (pH 7.4, 37 °C), observed by fluorescence detector at 370 nm of excitation and at 440 nm of emission. One micromolar pure CPT-20(*S*)-glycinate in DMSO solution (2.6 min, peak B) (i) and 1 min after dissolving CPT-20(*S*)-glycinate in PBS buffer (pH 7.4, 37 °C), peak C appeared (5.1 min) (ii) 1 h LC chromatogram with two additional peaks were distinguished being lactone form of CPT (6.7 min, peak D) and carboxylate form of CPT (2.1 min, peak A) and (iii) CPT-20(*S*)-glycinate and lactone and carboxylate form of CPT were identified by comparison of their HPLC retention times with that of reference standards. The experimental conditions were described in the text.

prodrug CPT-20(*S*)-glycinate ester in aqueous solutions at physiological condition results in the rapid formation of several degradants and eventually releases active CPT. A stacked plot of typical reversed-phase HPLC chromatograms as a function of time using fluorescence detection is presented in Fig. 3 which documents the instability of CPT-20(*S*)-glycinate ester in aqueous solution under physiological conditions of pH and temperature. The aqueous sample of CPT-20(*S*)-glycinate ester (peak B) was pure initially, as evidenced by the presence of only a single peak in DMSO. It should be mentioned, however, that immediately upon dissolution in PBS (pH 7.4), CPT-20(*S*)-glycinate ester generates an unknown peak (peak C), which was more hydrophobic than the CPT-20(*S*)-glycinate according to the elution order. Subsequently, the early eluting degradant (peak A) and late eluting degradant (peak D) appeared and identified as the carboxylate form of CPT and the lactone form of CPT, respectively. These initial identifications were made by comparison to the elution of standard material. A similar LC chromatogram was also observed when using UV detection. ESI–MS experiments (discussed later) suggested that the early eluting peak actually comprised two species. These two species were not differentiated by fluorescence or UV detector since they coeluted on the C18 column. CPT-20(*S*)-glycinate showed similar enhanced reactivity in human plasma and whole human blood (pH 7.4, 37 °C). No dramatic rate difference was observed between aqueous buffer and biological fluids which indicated that CPT-20(*S*)-glycinate underwent spontaneously chemical activation (i.e. non-enzymatic mechanism).

3.2. pH effect of degradation of the CPT-20(S)-glycinate ester

The influence of pH on the hydrolysis rate of the CPT-20(*S*)-glycinate ester was also evaluated and presented in Fig. 4. As it can be seen, the prodrug was stable at low pH and the rate of decomposition was accelerated at higher pH. Apparently, the activate drug release was controlled by pH. We also noticed that

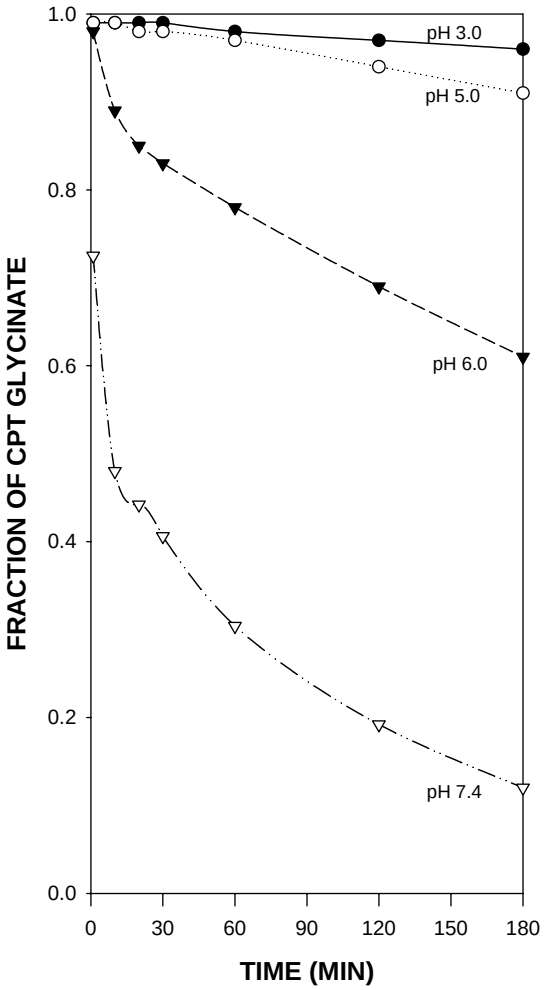

Fig. 4. Stability of CPT-20(*S*)-glycinate in different pH conditions. Stability profile was determined using HPLC methods. All experiments were conducted at pH 7.4 and 37 °C. Stability profile graph was constructed by plotting the fractional percent of CPT-20(*S*)-glycinate decayed over a time course. Fractional percentage of CPT-20(*S*)-glycinate was calculated based on the ratio of the peak area of analyte at 1, 10, 20, 30, 60, 120 and 180 min vs. the initial peak area. Each stability profile represents the average of at least three independent runs with the same sampling schedules. The standard deviation of each point is typically 5% or less.

the intermediate (peak C) could be converted back to starting material when the hydrolysis reaction under in physiological conditions was reverted by adjusting the pH immediately to 2. This suggested the existence of equilibrium between starting material and the intermediate.

3.3. LC–ESI–MS study the degradation of CPT-20(S)-glycinate

In order to gain a better understanding of this non-enzymatic, self-activating degradation pathway of the CPT-20(*S*)-glycinate hydrolysis reaction, LC–ESI–MS was employed to identify and characterize the structure of unknown species generated from the CPT-20(*S*)-glycinate ester in aqueous solution. In order to be compatible with electrospray interface and avoid non-volatile mobile phase components used in the previous HPLC assay, new LC methods were utilized and a microbore C18 column was used as described in experimental section to improve the sensitivity of LC–MS assay.

The LC–ESI–MS full-scan chromatogram of the hydrolyzed products of prodrug CPT-20(*S*)-glycinate ester is shown in Fig. 5. According to the retention behavior and in comparison to standard CPT-20(*S*)-glycinate; lactone and carboxylate form of CPT; peaks 1, 3 and 4 can be tentatively assigned as carboxylate form of CPT, CPT-20(*S*)-glycinate ester and lacone form of CPT. Interestingly, a detailed investigation of the MS spectrum of the peak 1 indicated another degradation product that was hidden under the large carboxylate form of CPT, this was evidenced by Fig. 6A and B. Fig. 6A shows the mass spectrum of the standard carboxylate form of CPT (MW 366) prepared by diluting CPT stock in pH 10 aqueous solution. The ions *m*/*z* 367 and 389 could be assigned as the protonated and sodiated molecular ions of carboxylate form of CPT, respectively (Table 1). By comparison, panel B shows the mass spectrum of peak 1 (same retention time) generated from the degradation reaction. The diagnostic product ions indicate a great deal of similarity with the standard carboxylate form of CPT due to the presence of $[\text{CPT carboxylate}+\text{H}]^+$ at *m*/*z* 367 and $[\text{CPT carboxylate} + \text{Na}]^+$ at *m*/*z* 389. However, the generation of *m*/*z* 406, 424 and 446 which were not observed in the MS spectrum of standard carboxylate form of CPT indicated the presence of an unresolved species which coeluted with carboxylate form of CPT. The structure of this previously unresolved species was proposed to be [2-hydroxy-2-(8-hydroxymethyl-9-oxo-9,11-dihydro-indolinizino[1,2-b]quinolin-7-yl)-butyrylamino]-acetic acid (TB-3, MW 423) (Scheme 1 for chemical structure). This structure is very similar to the carboxylate

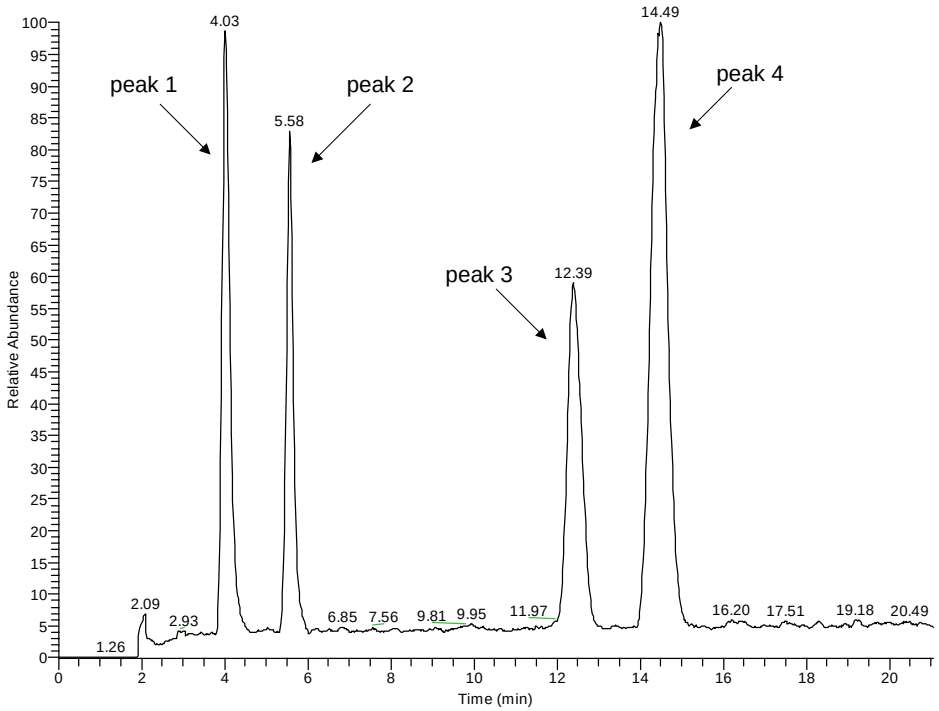

Fig. 5. Representative LC–ESI–MS total-ion current chromatogram of 5 μM CPT-20(*S*)-glycinate incubated in pH 7.4 aqueous solution for approximately 1.5 h at room temperature. CPT-20(*S*)-glycinate and lactone and carboxylate form of CPT were identified by comparison of their HPLC retention times and fragment patterns with that of reference standards. Conditions were described in the text.

form of CPT in that all are ring-opened structures and easily form zwitterions in water, which explains their early elution on the C18 reversed-phase column. Key product ions at *m/z* 424 $[M+H]^+$ and 446 $[M+Na]^+$ support the proposed structure. This conclusion was further supported by the presence of the fingerprint ions of *m/z* 406, which could be explained as TB-3 losing a water molecule. In a MS/MS experiment, the protonated precursor molecular ion *m/z* 424 was selected and collisionally dissociated with relative collision energy of 35% resulting in the product ion *m/z* 406 from loss of water (Fig. 6C). Additionally, we recently showed (unpublished data) that the coeluted species could be resolved by HPLC coupled with

Table 1
Summary of the observed retention times, mass values and fragment ions for the LC–ESI–MS analysis of the hydrolysis products of the prodrug CPT-20(*S*)-glycinate

Peak number	Retention time (min)	Protonated molecular ions	Observed fragment ions & attribution	Peak assignment & proposed structure*
Peak 1	4.03	367	*m/z* 389 $(M + Na)^+$ *m/z* 367 $(M + H)^+$ *m/z* 349 $(M + H\text{-}H_2O)^+$	CPT carboxylate
		424	*m/z* 446 $(M + Na)^+$ *m/z* 424 $(M + H)^+$ *m/z* 406 $(M + H\text{-}H_2O)^+$	TB-3*
Peak 2	5.58	406	*m/z* 428 $(M + Na)^+$ *m/z* 406 $(M + H)^+$ *m/z* 331 (-glycine)$^+$ *m/z* 303 (-glycine-CO)$^+$	CPT-20(*S*)-glycinate
Peak 3	12.39	406	*m/z* 428 $(M + Na)^+$ *m/z* 406 $(M + H)^+$ *m/z* 388 $(M + H\text{-}H_2O)^+$ *m/z* 303 (-103 a.m.u.)$^+$	TB-2*
Peak 4	14.49	349	*m/z* 371 $(M + Na)^+$ *m/z* 349 $(M + H)^+$ *m/z* 305 $(M + H\text{-}CO_2)^+$	CPT lactone

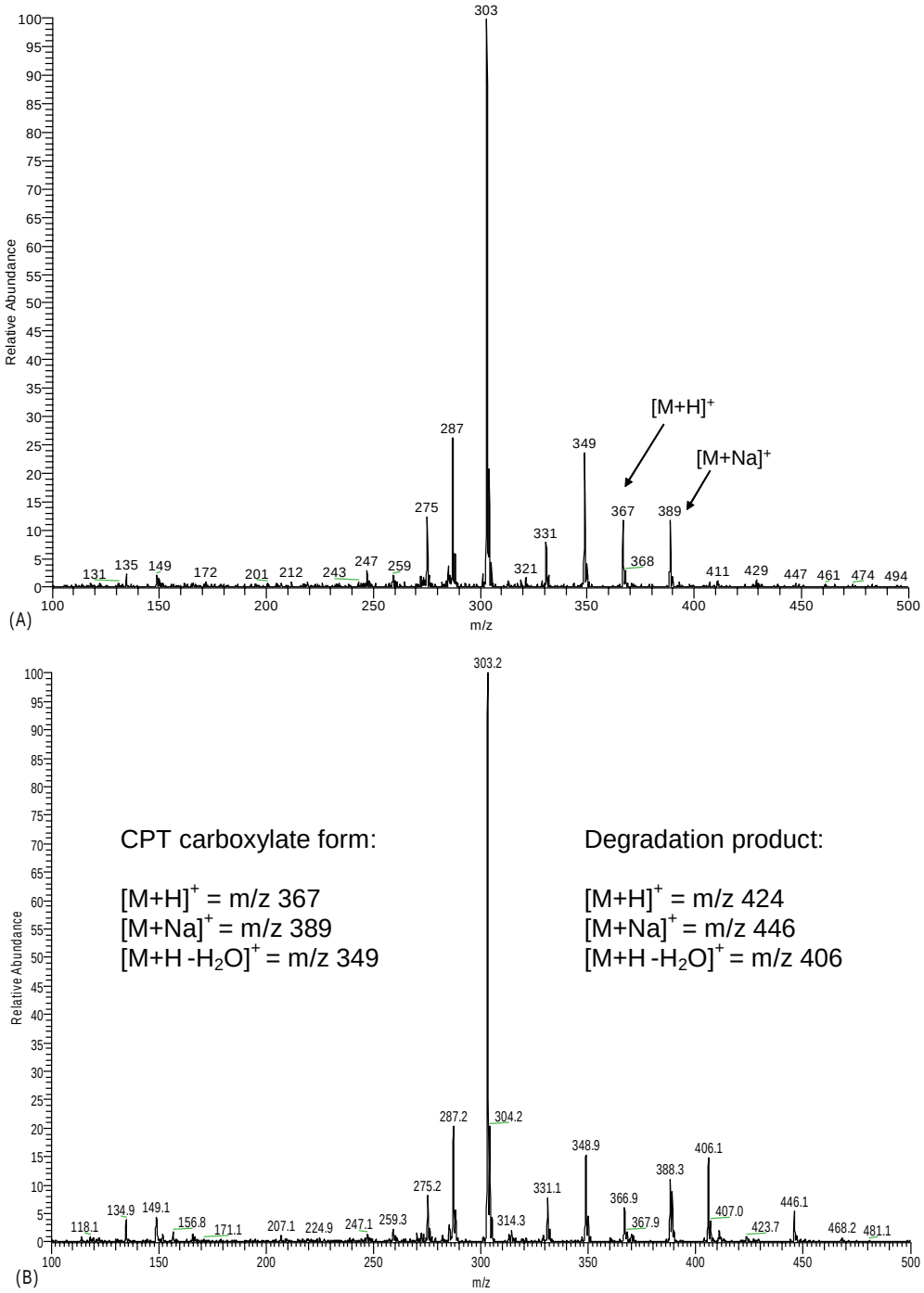

Fig. 6. The positive electrospray ionization–mass spectra of (A) standard carboxylate form of CPT (B) peak 1 from the degradation reaction of CPT-20(*S*)-glycinate in aqueous solution (C) MS/MS of *m*/*z* 424.

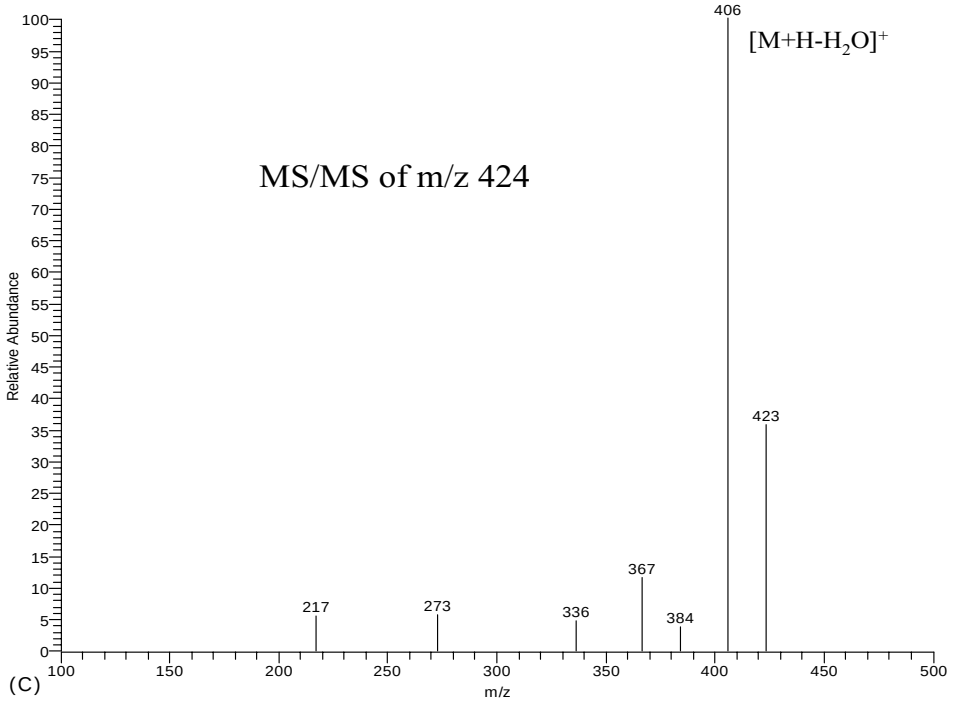

Fig. 6. (*Continued*).

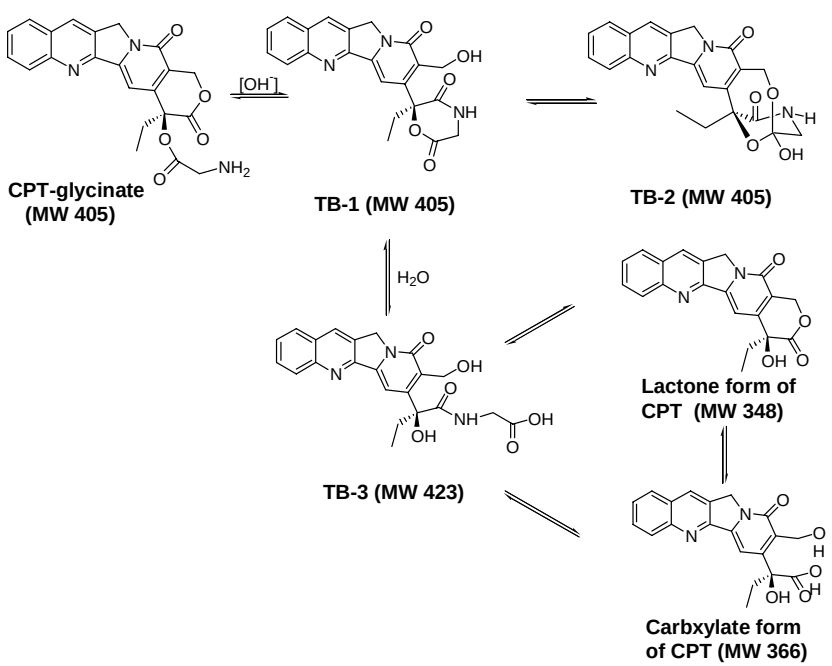

Scheme 1. The proposed degradation pathway of the CPT-20(*S*)-glycinate ester in aqueous solution.

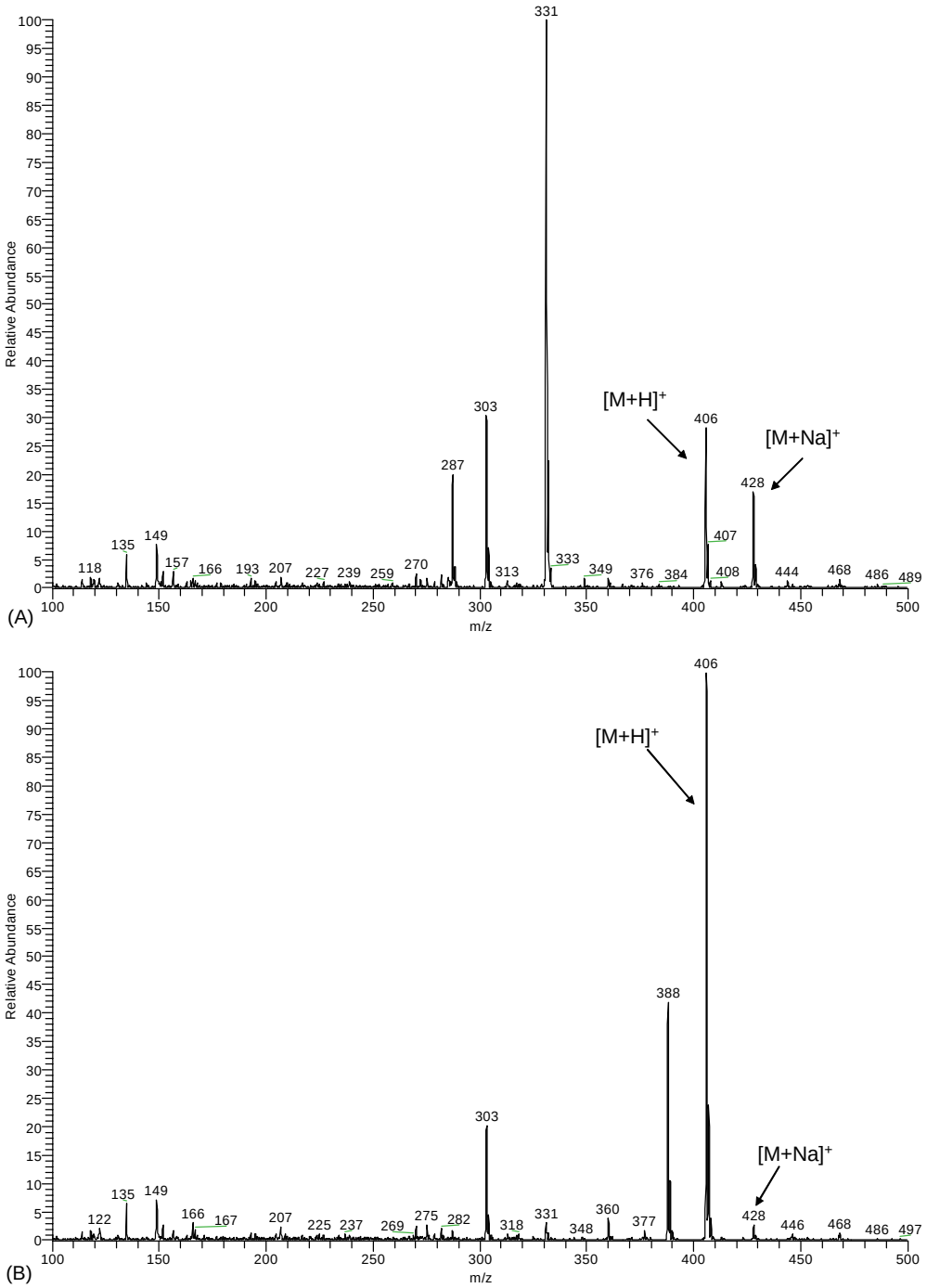

Fig. 7. The positive electrospray ionization-mass spectra of (A) peak 2 CPT-20(*S*)-glycinate (B) peak 3 intermediate species generated from the degradation reaction of CPT-20(*S*)-glycinate in aqueous solution, it has identical molecular mass as CPT-20(*S*)-glycinate, but different fragment ions and (C) MS/MS of *m*/*z* 406 of prodrug CPT-20(*S*)-glycinate (peak 2) and MS/MS of *m*/*z* 406 of intermediate species (peak 3).

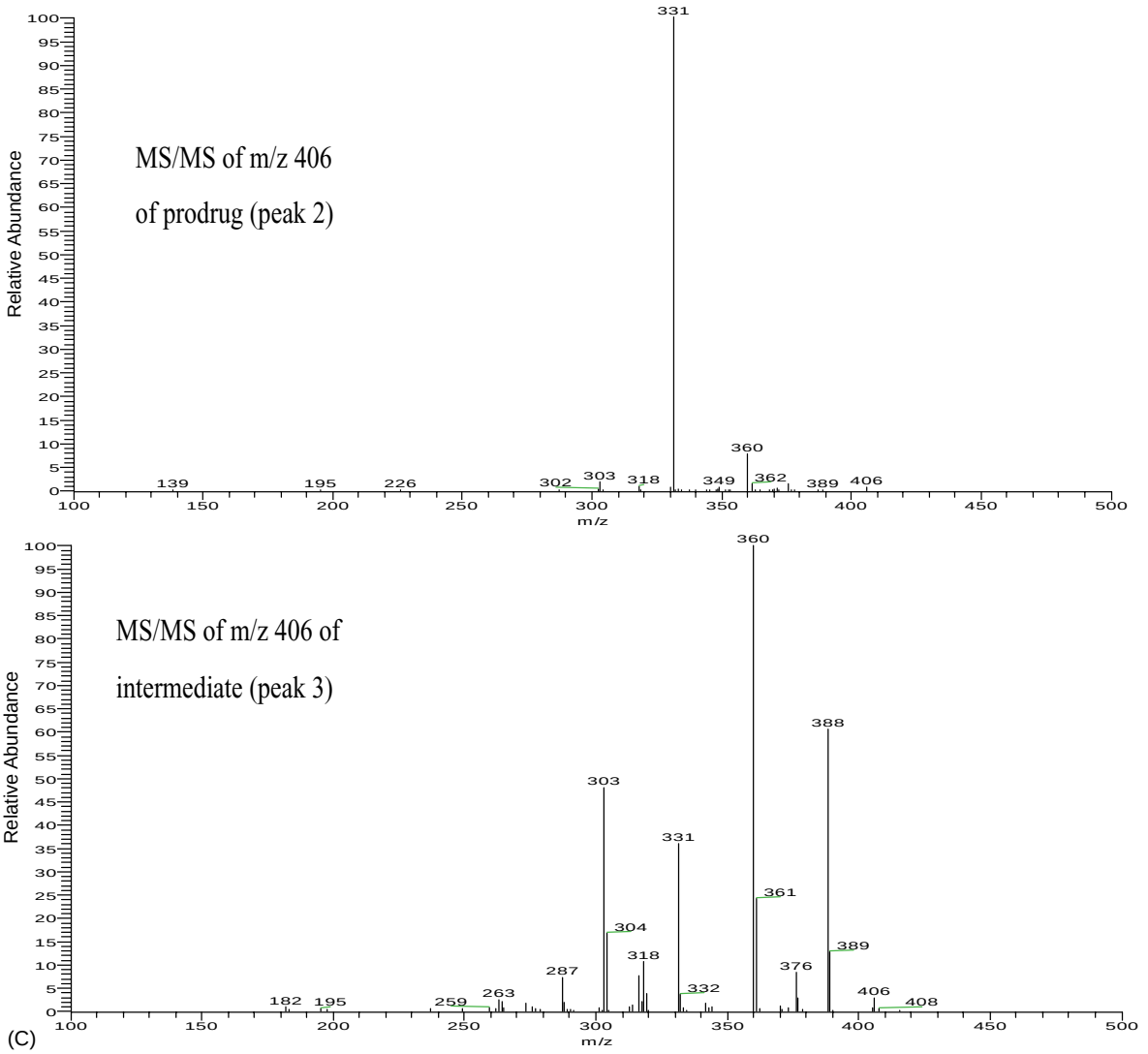

Fig. 7. (*Continued*).

fluorescence detection and MS detection respectively for 7 and 10 positions substituted analog DB-67 (7 - *t* - butyldimethylsilyl - 10 - hydroxy - camptothecin, Fig. 1) glycinate ester. This result further confirmed the involvement of coeluted degradation products. In conclusion, based on molecular mass as well as chromatographic retention information, peak 1 was tentatively assigned as the coelution of carboxylate form of CPT and ring opened degradation product TB-3.

More importantly, LC–ESI–MS results provide important information on the identity of intermediate species (peak 3) generated in the degradation process. Full scan mass spectra of peaks 2 and 3 (Fig. 7A and B) indicate that the intermediate has the same molecular mass as the prodrug (CPT-20(*S*)-glycinate), but a substantially different fragmentation pattern. Fig. 7A shows the mass spectrum of CPT-20(*S*)-glycinate in a pH 7.4 aqueous solution. Exactly the same mass spectrum was observed for CPT-20(*S*)-glycinate in a pH 3 aqueous solution, where no hydrolysis occurred confirming that peak 2 was intact CPT-20(*S*)-glycinate. Ions *m/z* 406 $[M + H]^+$ and *m/z* 428 $[M + Na]^+$

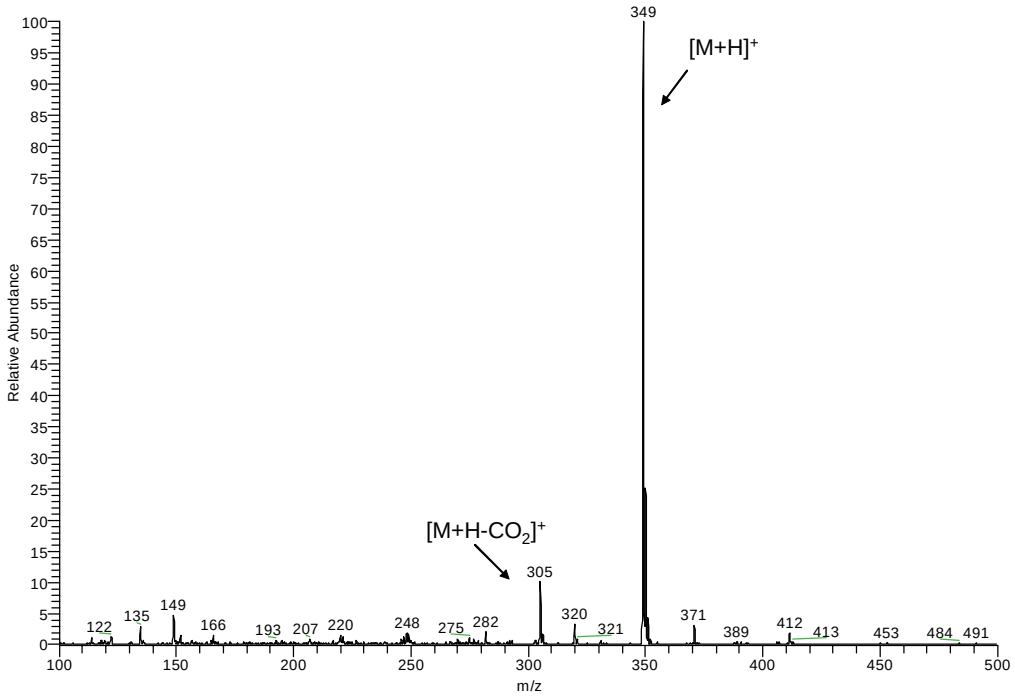

Fig. 8. The positive electrospray ionization-mass spectrum of peak 4 lactone form of CPT.

are consistent with the prodrug CPT-20(*S*)-glycinate (MW = 405). Additionally, diagnostic fragment ions *m*/*z* 331 (100% relative abundance) and *m*/*z* 303 (30% relative abundance) were observed. However, the full scan mass spectrum of peak 3 (Fig. 7B) indicated the intermediate had a molecular mass of 405 and was isomeric with CPT-20(*S*)-glycinate, as evidenced by the appearance of ions *m*/*z* 406 $[M + H]^+$ and *m*/*z* 428 $[M + Na]^+$. In sharp contrast with the starting material, the full scan mass spectrum of peak 3 also included diagnostic fragment ions at *m*/*z* 388 (40% relative abundance) and 303 (20% relative abundance). To further differentiate the structures of prodrug CPT-20(*S*)-glycinate and intermediate species, tandem mass spectrometry of the respective protonated molecular ions was employed. Dramatically different product ion were obtained (Fig. 7C) clearly delineating the structural differences between the two compounds.

The lactone form of CPT peak (peak 4, MW 348) fragmentation pattern is exactly the same as the reference sample (Fig. 8). The product ions present in the MS spectrum of CPT lactone includes: $[M + H]^+$ *m*/*z* 349, $[M + Na]^+$ *m*/*z* 371, and a peak of *m*/*z* 305 generated from the neutral loss of CO_2. Table 1 summarizes the observed mass values and fragmentation patterns of each species generated from hydrolysis reaction of the prodrug CPT-20(*S*)-glycinate in aqueous solution.

3.4. Proposed degradation pathway

On the basis of the obtained experimental evidence, the intramolecular cyclization reaction pathway and intermediates structures are proposed in Scheme 1. In view of the well-documented basicity and nucleophilicity of the amine, we envision the mechanism for the transformation to proceed via a base catalyzed nucleophilic attack of the lactone carbonyl electrophile by the terminal amine group and formation of transient species TB-1 (a six-membered morpholine-2, 5-dione ring with lactam moiety). This

transient species quickly converts to TB-2 (intermediate peak 3) and TB-3 (one of coeluents of peak 1) via a second intramolecular cyclization and competitive intermolecular reaction. The lactone form and carboxylate form of CPT are subsequently generated from TB-3 through an intramolecular and intermolecular reaction. Although these mass spectral data are consistent with the proposed structure, additional structural assignment by NMR and isotope labeling experiments are required to confirm these assignments. We are currently investigating this hypothesis further, the results of which will be reported in due course.

In conclusion, we have compared the stability of prodrugs camptothecin-20(*S*)-acetate and camptothecin-20(*S*)-glycinate in aqueous solutions and biological fluids. For the prodrug camptothecin-20(*S*)-glycinate which contains the terminal amine, rapid and essentially complete decomposition occurred, resulting in formation of degradation intermediates and eventually release of active camptothecin agent. The results are presented may be of clinical importance because 20(*S*)-glycinate esters of CPT and its more potent analogues have been examined in vivo against MX-1 and MDA-231 human tumor xenografts [5]. Understanding of parent camptothecin release mechanism from prodrug 20(*S*)-glycinate esters of CPT will eventually help us to develop novel non-enzymatic, self-activating camptothecin prodrugs for drug delivery and tumor targeting.

Acknowledgements

This work was supported by NIH CA 63653 grant (to T.G.B). We also acknowledge University of Kentucky Mass Spectrometry Facility.

References

[1] R. Vishnvvajjala, A. Garzon-Aburbey, US Pat. Appl., United States Department of Health and Human Services, USA, 1990, p. 21.
[2] M.E. Wall, M.C. Wani, A.W. Nicholas, G. Manikumar, C. Tele, L. Moore, et al., J. Med. Chem. 36 (1993) 2689–2700.
[3] Y.H. Hsiang, L.F. Liu, Cancer Res. 48 (1988) 1722–1726.
[4] Y.H. Hsiang, L.F. Liu, M.E. Wall, M.C. Wani, A.W. Nicholas, G. Manikumar, et al., Cancer Res. 49 (1989) 4385–4389.
[5] R.M. Wadkins, P.M. Potter, B. Vladu, J. Marty, G. Mangold, S. Weitman, et al., Cancer Res. 59 (1999) 3424–3428.
[6] X. Liu, B.C. Lynn, J. Zhang, L. Song, D. Bom, W. Du, et al., J. Am. Chem. Soc. 124 (2002) 7650–7651.
[7] D.L. Warner, T.G. Burke, J. Chromatogr. B 691 (1997) 161–171.
[8] R.P. Hertzberg, M.J. Caranfa, K.G. Holden, D.R. Jakas, G. Gallagher, M.R. Mattern, et al., J. Med. Chem. 32 (1989) 715–720.
[9] J. Fassberg, V.J. Stella, J. Pharm. Sci. 81 (1992) 676–684.
[10] T.G. Burke, Z. Mi, J. Med. Chem. 37 (1994) 40–46.
[11] L.P. Rivory, J. Robert, Pharmacol. Ther. 68 (1995) 269–296.
[12] H. Zhao, C. Lee, P. Sai, Y.H. Choe, M. Boro, A. Pendri, et al., J. Org. Chem. 65 (2000) 4601–4606.